

# Nanopottery: Coiling of Electrospun Polymer Nanofibers

Ho-Young Kim,<sup>\*,†</sup> Minhee Lee,<sup>†</sup> Kun Joong Park,<sup>†</sup> Sungho Kim,<sup>†</sup> and L. Mahadevan<sup>\*,‡</sup>

<sup>†</sup>School of Mechanical and Aerospace Engineering, Seoul National University, Seoul 151-744, Korea, and <sup>‡</sup>School of Engineering and Applied Sciences and Kavli Institute for Bionano Science and Technology, Harvard University, Cambridge, Massachusetts 02138

**ABSTRACT** We show that a nanoscale polymer solution electrojet can coil to form free-standing hollow pottery as the jet is focused onto a sharp electrode tip. A scaling law is given based on the balance of the electrostatic compression force and the elastic resistance to predict the coil radius and frequency as the functions of relevant physical parameters. The structures formed by the nanofibers can be used in diverse fields of nanotechnology, for example, as nanomagnets, bioscaffolds, and nanochannels.

**KEYWORDS** Coiling, electrospinning, nanofiber, jet stability, pottery, elasticity

The buckling, folding, and coiling of thin sheets and filaments of solids and fluids take place on length scales spanning several orders of magnitude, in phenomena ranging from orogenesis in geophysics to materials processing and soft-matter physics. For example, when an elastic rope is fed uniformly toward a horizontal plane, it first buckles and eventually coils into a spool that is deposited onto the plane.<sup>1</sup> A similar phenomenon also occurs when a slender viscous fluid jet impinges onto a horizontal plane and leads to the deposition of a liquid rope coil.<sup>2</sup> In either case, although the scale of the coil and the speed of coiling are determined by the balance between the internal elastic or viscous forces that resist deformation and a combination of inertia and gravity, the basic phenomenology is a consequence of geometry which favors bending deformations over stretching modes.

Here, we consider the spontaneous coiling of nanometric polymeric filaments that are electrospun onto a substrate to form regular cylindrical spools. When a polymer solution drop hanging from a capillary needle tip is subjected to a strong electrical field, a nanoscale jet is drawn out<sup>3</sup> and is attracted to the electrode. However, a bending instability of the electrified jet due to surface charges commonly leads to the chaotic deposition of nanofibers.<sup>4</sup> Attempts to stabilize the jet by reducing the distance between the plate ground and the liquid drop<sup>5</sup> or by placing a sharp ground tip adjacent to a collector plate<sup>6</sup> still resulted in the chaotic deposition of fibers on a stationary plate as shown in Figure 1. In the experiments, the nanofibers were electrospun onto (A) a conducting Al plate only 2 mm from the capillary tip and onto (B) a glass sheet at the same location as the Al plate with a sharp electrode tip underneath.

To prevent the jet instability, we finally used a sharp electrode tip near the liquid drop source with a strongly focused electrical field at the ground. This caused a stable jet to impinge on the tip and buckle and coil to yield a free-standing cylindrically spooled structure. Figure 2A shows the experimental setup, consisting of a syringe pump that supplies a polymer solution of poly(ethylene oxide) (PEO, molecular weight = 300000) to a metal capillary, a stainless steel conical ground with 50  $\mu\text{m}$  in apex diameter situated 2 mm from the drop, a high voltage source, and a high-speed

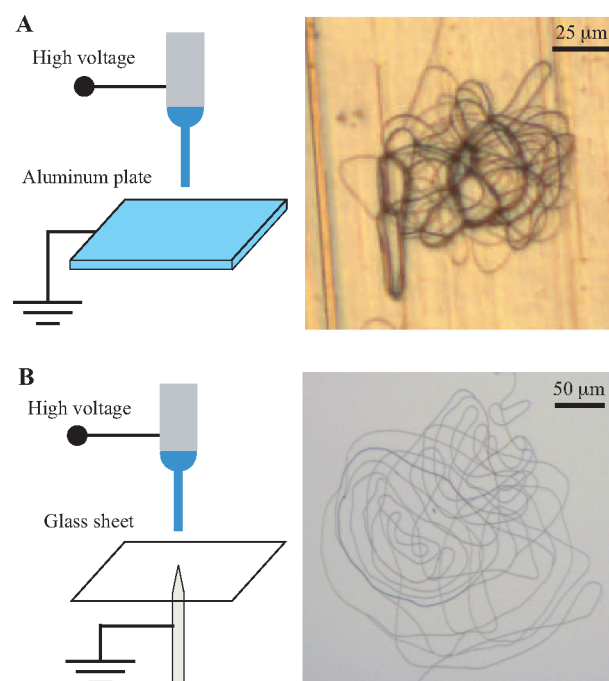


**FIGURE 1.** Chaotically deposited nanofibers as electrospun by the previously suggested focusing schemes. (A) Using an Al plate close to the capillary tip with the voltage difference of 1 kV. (B) Using a glass sheet with a sharp ground tip underneath. In both experiments, the jet duration was identically 0.7 s. Other experimental conditions are identical to those employed to yield the result of Figure 2.

\* To whom correspondence should be addressed, hyk@snu.ac.kr and lm@seas.harvard.edu.

Received for review: 03/8/2010

Published on Web: 05/20/2010

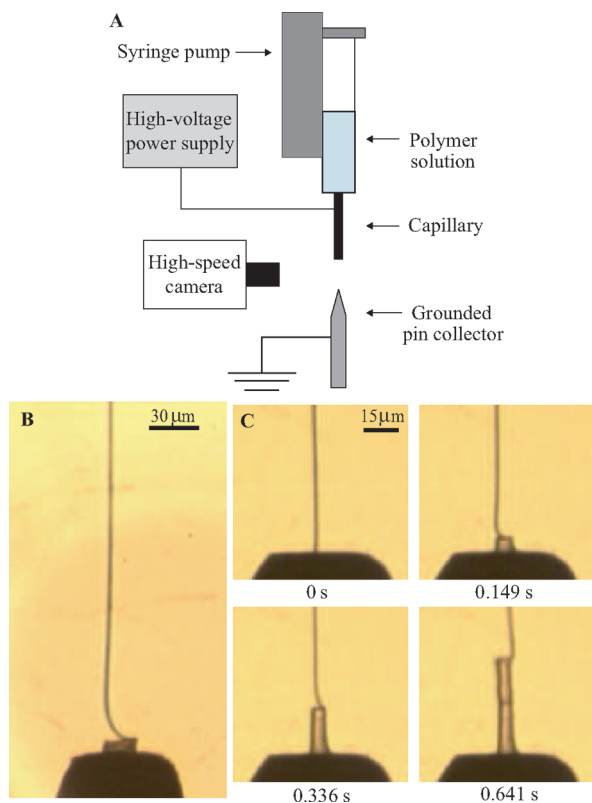


**FIGURE 2.** Experimental images of nanocoiling polymer fiber. (A) Schematic of the experimental apparatus. (B) A snapshot of a nanojet with 470 nm in final constant radius. (C) High-speed sequential images of a nanocoiling process that yields a free-standing hollow cylinder.

camera. In our experiments performed at room temperature and normal atmospheric pressure, an electrical jet is emitted from the drop when the electrical field strength exceeds approximately  $1.2 \times 10^6$  V/m. The velocity and radius of the jet are functions of the viscosity of the drop, which depends on the initial PEO concentration (we used 6, 10, and 14 wt % of aqueous PEO solutions), the rate of evaporation, and the applied field, and yields a range of velocities,  $U \in [1.5 \text{ } 30] \text{ mm/s}$  and radii,  $r \in [75 \text{ } 500] \text{ nm}$ . As the solvent of the solutions, we used water purified by reverse osmosis. The permittivity of the initial aqueous solutions of PEO was measured, via open-ended sensors and reference liquid calibration,<sup>7</sup> to be  $6.53 \times 10^{-10}$ ,  $6.24 \times 10^{-10}$ , and  $5.97 \times 10^{-10}$  F/m for PEO concentrations of 6 %, 10 %, and 14 %, respectively.

Although the polymer solution is initially liquid, it starts to dry upon emerging as a drop of diameter  $d \sim 1 \text{ mm}$  from the capillary and continues to dry as the jet flies through air. In our experiments, the solvent is estimated to have ample time to diffuse toward the fiber interface and evaporate into ambient air (Supporting Information). Hence, the jet is effectively a solid by the time it impinges on the target, as evidenced by the constant diameter of the jet shown in Figure 2B, and may be modeled as a thin elastic filament of radius  $\sim 50 \text{ nm}$  even as it coils onto the tip ground. Figure

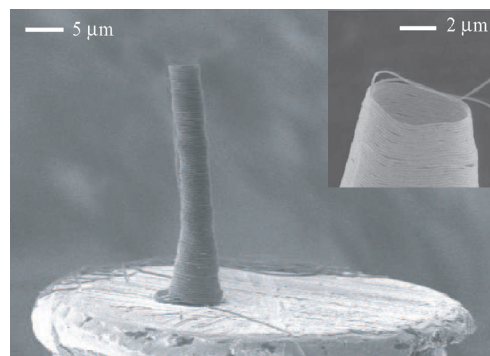


**FIGURE 3.** SEM images of the hollow coiled structure built on an apex of the stainless steel conical tip.

2C shows sequential images of the formation of a three-dimensional coiled structure of radius approximately  $3 \mu\text{m}$  and height  $40 \mu\text{m}$  as the jet whirls at a rate of  $\sim 10000 \text{ rpm}$ , so that the entire structure is built in less than a second. In Figure 3 we show scanning electron microscopy images of hollow free-standing cylinders that might well have been shaped on a (nano) pottery wheel.

To characterize the coiling phenomenon and predict the radius of the coil  $R$  on relevant physical parameters, we consider the dominant forces acting on the fiber. The electrostatic force per unit fiber length  $F_e$  is scaled as  $F_e \sim q_s r E$ , where the electrical field strength  $E \sim V/L$  with  $V$  being the electrical potential difference between the drop and the ground, separated by the distance  $L$ . The surface charge density  $q_s$  is scaled as  $q_s \sim \epsilon_0 E$ , where  $\epsilon_0 = 8.854 \times 10^{-12}$  F/m is the permittivity of free space, provided that the fiber permittivity  $\epsilon \gg \epsilon_0$ .<sup>8</sup> The inertial forces scale as  $F_i \sim \rho r^2 \Omega^2 R$ , where  $\rho$  is the fiber density and  $\Omega$  the angular frequency of coiling, and the gravitational forces per unit length scale as  $F_g \sim \rho g r^2$ , where  $g$  is the gravitational acceleration. Using typical experimental parameter values ( $r \approx 100 \text{ nm}$  and  $\rho \approx 1.21 \times 10^3 \text{ kg/m}^3$ ), we find  $F_i/F_e \sim 10^{-5}$  and  $F_g/F_e \sim 10^{-4}$  so that  $F_i$  and  $F_g$  are negligibly small compared with  $F_e$ .

Then the spooling or coiling radius is determined by a balance between the electrostatic torque  $F_e R^2$  and the elastic torque  $YI/R$ ,<sup>9</sup> where  $Y$  is Young's modulus of a fiber and  $I$  the area moment of inertia ( $\sim r^4$ ), so that

$$R \sim \left( \frac{Y}{\epsilon_0 E^2} \right)^{1/3} r \quad (1)$$

The angular frequency of coiling  $\Omega$  follows from mass conservation since  $\Omega R = U$ , so that

$$\Omega \sim \frac{U}{r} \left( \frac{\epsilon_0 E^2}{Y} \right)^{1/3} \quad (2)$$

To test this prediction, we need to measure Young's modulus of a nanofiber as a function of solute (PEO) con-

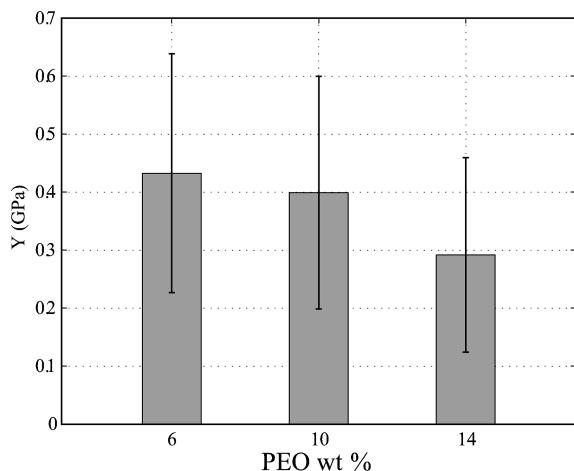


FIGURE 4. The averaged Young moduli of nanofibers with different PEO concentrations.

centration, a critical factor in determining the elasticity of these polymeric materials which move through a glass transition as a function of solute concentration. We deflected individual fibers hanging over a microtrench of width  $30\ \mu\text{m}$  and depth  $3\ \mu\text{m}$  (formed by deep etching of a silicon wafer) using an atomic force microscope (AFM) to measure  $Y$ , as delineated in Supporting Information. The measurement results allow us to find the dependency of the average modulus  $Y$  on PEO concentrations as shown in Figure 4.

The scaling law (1) states that the coil radius increases with fiber radius and/or with the electric field. In Figure 5 we plot the coil radius for a range of PEO concentrations in the solvent and the field  $E$ , as a function of the parameter  $(Y/\epsilon_0 E^2)^{1/3} r$ , and see that the straight line fits  $R \sim 0.05(Y/\epsilon_0 E^2)^{1/3} r$ , consistent with our simple scaling predictions.

In summary, we have shown that coiling of nanoscale fibers can arise as an electrospun polymer solution jet is focused onto a sharp electrode tip, leading to a stable hollow helical structure. A simple scaling law captures the physics of the process and enables us to start thinking about the control of the coil geometry using experimental parameters. The regular geometry of coiling microstructures may be of use in nanoscale magnets, in building nanotextured surfaces for bioscaffolds and nanochannels, and in other functional structures. An array of electrode target spots on an insulating substrate that are turned on sequentially may provide a viable solution to fabricate two-dimensional arrays of coiling microstructures because it can prevent electric field interference. Further study for fabrication of multiple spools on an

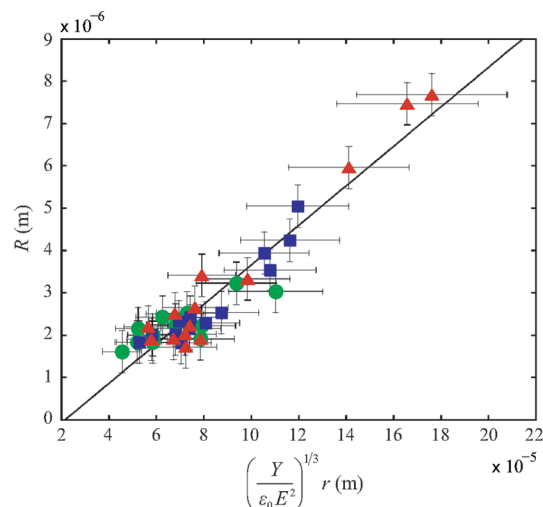


FIGURE 5. Coil radii plotted according to the scaling law (1). Circles, squares, and triangles correspond to 6, 10, and 14% of aqueous PEO solutions, respectively.

array of target spots using different solutions will be crucial in realizing the wide application of this nanocoiling process.

**Acknowledgment.** This work was supported by KOSEF (R01-2006-000-10444-0) and KRF (412-J03001), and administered by SNU-IAMD.

**Note Added after ASAP Publication.** This paper published ASAP May 20, 2010 without the Acknowledgment section; the corrected version published ASAP May 25, 2010; L. Mahadevan's affiliation was updated on June 9, 2010.

**Supporting Information Available.** Estimation of solvent evaporation and measurement of Young's modulus. This material is available free of charge via the Internet at <http://pubs.acs.org>.

## REFERENCES AND NOTES

- (1) Mahadevan, L.; Keller, J. B. *Proc. R. Soc. London, Ser. A* **1996**, 452, 1679.
- (2) Mahadevan, L.; Ryu, W. S.; Samuel, D. T. *Nature* **1998**, 392, 140. Mahadevan, L.; Ryu, W. S.; Samuel, D. T. *Nature* **2000**, 403, 502.
- (3) Reneker, D. H.; Yarin, A. L. *Polymer* **2008**, 49, 2387.
- (4) Reneker, D. H.; Yarin, A. L.; Fong, H.; Koombhongse, S. *J. Appl. Phys.* **2000**, 87, 4531.
- (5) Sun, D.; Chang, C.; Li, S.; Lin, L. *Nano Lett.* **2006**, 6, 839.
- (6) Yu, J.; Qiu, Y.; Zha, X.; Yu, M.; Yu, J.; Rafique, J.; Yin, J. *Eur. Polym. J.* **2008**, 44, 2838.
- (7) Nyshadham, A.; Sibbald, C. L.; Stuchly, S. S. *IEEE Trans. Microwave Theory Tech.* **1992**, 40, 305.
- (8) Haus, H. A.; Melcher, J. R. *Electromagnetic Fields and Energy*; Pentice-Hall: Englewood Cliffs, NJ, 1989.
- (9) Landau, L. D.; Lifshitz, E. M. *Theory of Elasticity*, 3rd ed.; Butterworth-Heinemann: London, 1986.